RSC Advances

COMMUNICATION

View Article Online
View Journal | View Issue

Cellulose nanofiber assisted deposition of titanium dioxide on fluorine-doped tin oxide glass

Cite this: *RSC Adv.*, 2014, **4**, 987

Received 24th July 2013
Accepted 4th November 2013

DOI: 10.1039/c3ra43818j

www.rsc.org/advances

Jitendra K. Pandey,[a] Jung-Oh Choi,[a] Hyun-Taek Lee,[a] Chung-Soo Kim,†[a] Hyun-Joong Kim,[b] Sera Jeon[b] and Sung-Hoon Ahn*[a]

Microspores, highly ordered, 300–340 nm thick blocks of titanium dioxide (TiO_2) nanoparticles (5–10 nm) were deposited on fluorine-doped tin oxide (FTO) glass by using low concentration of cellulose nanofibers from bacterial origin, through sol–gel process followed by spin coating.

Introduction

Fabrication of material through templating from structures of biological origin by taking advantage of their extraordinarily unique functionality, porosity and hierarchy is a growing area of research ensuring the controlled synthesis of membranes, films and particles.[1–12] Highly stable, biocompatible, nontoxic, photo reactive, cost effective and semiconducting TiO_2 nanoparticles based materials has been of immense importance because of its application in photo-catalysis, UV blocker, sublimation material, sensors, microelectronics, energy harvesting, optical and medical applications.[3–15] The efficiency of TiO_2 based materials depend on phase (anatase or rutile), size, shape and porosity of films and particles. Mesoporus TiO_2 has been synthesized by using biological templates such as yeast cells,[1] leaf,[2] bamboo[3] eggshell[4] bacterial thread[5] insect wings[6] pollen grains[7] wood[8] echinoid skeleton[9] cellulose.[10] Deposition of TiO_2 nanoparticles on FTO glass is one of the intense areas of research due to its direct applicability for development of energy harvesting devices based on solar energy where TiO_2 nano-crystalline semiconductor oxide, responsible for the transportation of electron through the surface or bulk of TiO_2 nanoparticles, to circuit after absorbing dye molecules; largely dictate the efficiency of product. The main challenges are the balance between large and small particles that allow proper light scattering, thickness and porosity of the films for higher absorption of dye on particle surface. The present approach is aimed to construct an assembled surface consisting TiO_2 blocks of nanoparticles, surrounded by nanoparticles.

To the best of our knowledge, bio templating directly on the FTO glass, assisted with cellulose nanofibers from bacterial origin has not been reported so far.

Nano-cellulose (also abbreviated as cellulose whiskers, nano-crystalline cellulose, cellulose nanofibers, nano-fibrillated cellulose), found in the plant cell wall is highly crystalline in nature situated inside the amorphous matrix of hemicellulose, lignin and other cementing material.[14] Bacterially derived nano-cellulose (BC) has an advantage in terms of its purity because absence of hemicellulose, lignin, pectin, wax *etc.*, which is present in plant derived nano-cellulsoe. Additionally, three dimensional networks of micro-fibrils in BC, biocompatibility, higher toughness permit to use them in the fields of medicine, water treatment, pharmaceuticals and drug delivery systems, template for fabrication of verity of metal oxide nano particles and wires[11–15] in cost effective ways. Our purpose was to use the ribbons shaped BC for the fabrication of TiO_2 meso/microporus film by sol gel process. Further, a very low amount of cellulose nanofibers was used during the process which provides the cost effectiveness in comparison of process where large amount of bacterial cellulose required for templating.

Experimental

BC was cultivated by *Gluconacetobacter xylinus* in a statically cultured Hestrin and Schramm medium as reported elsewhere.[16] The medium containing cell colony, was kept for 10 days at 30 °C after sterilizing at 121 °C for 1.5 h. The remaining cells on the surface pellicle were removed after thoroughly washing by de-ionized water and sodium hydroxide solution (2% wt%) followed by 20 minutes treatment in bleaching solution (sodium chlorite solution, 2.0% w/w in

[a]*School of Mechanical & Aerospace Engineering, Building 301, Room 1205, Seoul National University, Seoul, Korea 151-744. E-mail: ahnsh@snu.ac.kr; Fax: +82-2-8889043; Tel: +82-2-880-7110*

[b]*College of Agricultural and Life Sciences, Seoul National University, Seoul, Korea 151-744*

† Present affiliation is Research Laboratory of Electronics, Massachusetts Institute of Technology, USA.

water, mixed with equal amount of acetate buffer and diluted with 2 liter of distilled water). Pellicle was put under high sonication for 30 minutes at 9 × 10% cycle every 7.5 minutes. After filtration and washing with water the separated fibers were again dispersed in water by sonication for 10 minutes in similar conditions. The concentration of fibers was adjusted to 0.5% after solvent exchange in the dry ethanol. 10 ml of 1 M HCl was added in the suspension and stirred overnight at room temperature. Titanium tetraispropoxide ($Ti(OPr)_4$) or TTP, precursor was applied without further purification. TiO_2 nano powder was in anatase form with surface area of around 190–290 $m^2\ g^{-1}$, 5–20 nm particle size. All chemicals were used as received. The sol was prepared by 1 : 15 : 15 : 1.5 molar ratio of TTP : H_2O: EtOH : HNO_3. The milky slurry turns to transparent after stirring for 6 h. The cellulose nanofiber suspension was mixed drop wise in the TiO_2 nano-colloids at 80 °C. After complete mixing, suspension was stirred for 10 h where it converted to semi viscous paste. 1 drop of solution was spin coated at 6000 rpm and the process was repeated 3 times and put for heating at 500 °C at the rate of 5 °C per minute for 2 h. The samples were characterized by Scanning Electron Microscopy (SEM) through JEOL 7600F microscope at an accelerating voltage of 5 kV. All the samples were pre-coated with a homogeneous gold layer (purity 99.99%) by ion sputtering to eliminate electron charging. Transmission electron microscopy (TEM) was employed to observe the nanoparticle after deposition by Carl Zeiss energy-filtered transmission electron microscope, LIBRA 120, operated at 120 KV. The study of crystal structure was done by X-ray diffraction measurements on Bruker advanced consisted Cu Kα (λ = 1.542 Å) operated at 40 KV and 40 mA.

Results and discussion

The morphological analysis of BC is illustrated in the Fig. 1, that shows closely packed ribbon shaped fibers varying from 20 to 100 nm diameters piled above one another and entangled in criss crossing pattern. After treatment with sodium hydroxide, sodium chlorite and sonication, the agglomeration was destroyed due to breakage of many inter and intra molecular hydrogen bonds present in higher degree inside untreated BC[17] as well as removal of non-cellulosic materials in the form of nucleic acids, proteins from bacterial cell and colonies of bacteria. The sonication treatment was carried out to loosen the densely packed network and 0.5% (wt%) concentration of BC suspension was added into TTP colloid solution. The lowered concentration of bleaching and alkali treatment was conducted to avoid the change in crystal structure of BC from cellulose I to cellulose II as cellulose I polymorph have better mechanical properties.[18] The morphology of the spin coated and calcinated samples is presented in Fig. 2. The films formed shows the block of agglomerated TiO_2 nanoparticles. The big (300–340 nm thickness) blocks were results from decomposition of cellulose nano-ribbons leaving behind the agglomerated blocks of TiO_2 nanoparticles. More than 85% of the deposited TiO_2 in examined SEM images have thickness 340 nm which was reasonably uniform.

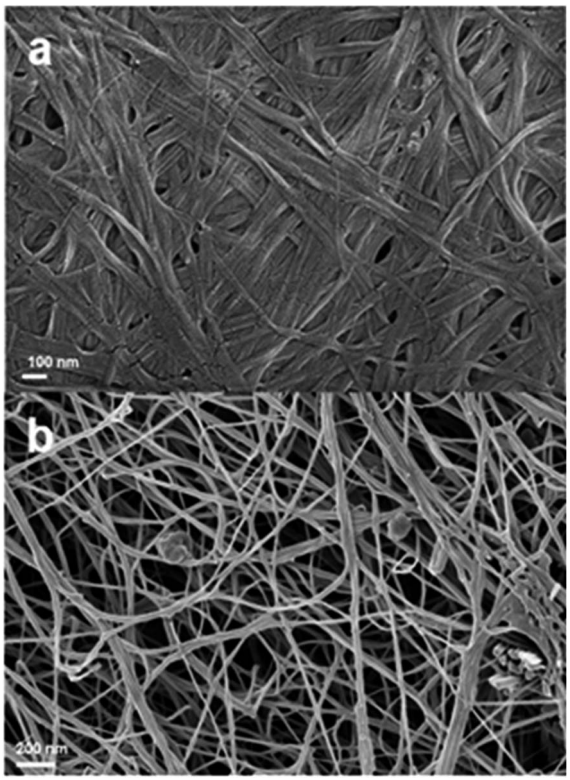

Fig. 1 SEM micrographs of cellulose (a) before (b) after sonicaton.

The intra particles distance was around 1.2 μm which was strong indication of cellulose nanofibers agglomeration upon water evaporation which forms the micro level bundles. The inset SEM image of these blocks further confirms the growth of blocks by deposition of TiO_2 nanoparticles. The assumption fueled by observation of TEM images showing the presence of nanoparticles of 10–15 nm near the edges of flakes.

Such type of structure must arise by the presence of nano dimensional fibres of BC in the system. As soon as reaction proceeds, the whole solution tend to become viscous through the evaporation of solvents, allowing the attraction of TTP toward nano-fibers due the presence of surrounded water layers where hydrolysis reaction may takes place. The particle formed was covered by cellulose chains to form inorganic-biopolymer composites stabilized by mainly physical quenching between cellulose chains.

The structural characterization was carried out by monitoring XRD spectra of specimens in Fig. 3. Peaks at 25.2, 35.6, 47.6, 64.2 and 69.9, 2-theta degree were indicating the presence of anatase form, representing (101), (103) (004) (200) (105) (204) (116) plane respectively.[19]

However, detectable peak at 38.4 (111) and 51.2 may be used as representation of rutile form of TiO_2 and FTO substrate respectively. Thus, tetragonal crystallization of mixed anatase and rutile form during particle formation demonstrating the polycrystalline nature of nano-particles. It has been observed that at higher temperature phase evolution can transform anatase to rutile form owing to the higher stability of the later.[20] In the present system, the dominant sharp peak of (101) reflects

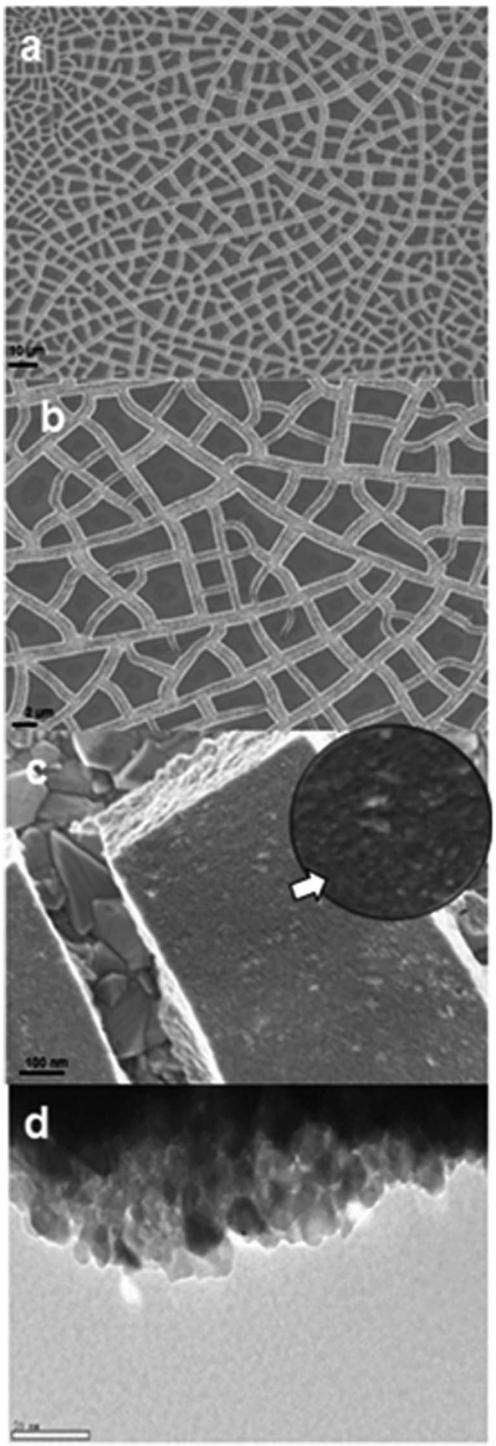

Fig. 2 SEM images of deposited TiO_2 particle (a), (b), (c) shows morphology at different magnifications. (d): TEM image of particles.

the presence of major anatase form of TiO_2 in the deposited film. The particle size was further confirmed by Scherrer formula through analysis of (101) reflection which exhibited the size of particle 40 nm. In general, the growth process of nano-crystalline anatase is mainly governed by the sintering of single crystals within the agglomerate and finally original agglomerate transform to larger single crystals.[21]

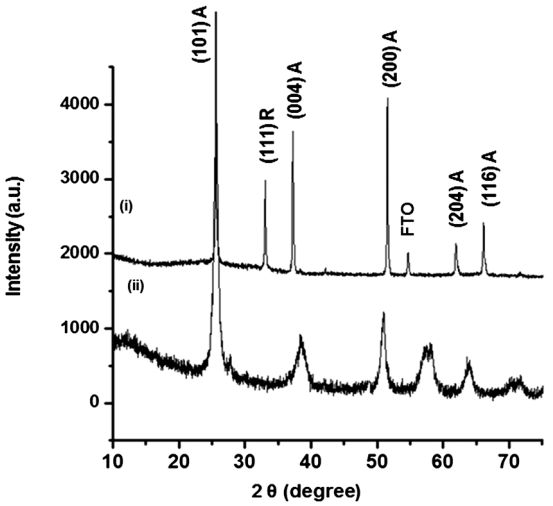

Fig. 3 XRD of specimens (i) deposited TiO_2 nanoparticles (ii) TiO_2 powder.

The high porosity and large surface area of TiO_2 films is one of the most important decisive factors for performance of TiO_2 photo-electrode.[22] To accelerate this property, the deposited blocks were further reinforced by TiO_2 nanoparticles and 0.02% (wt%) suspension (20 minutes sonication in isopropyl alcohol 1 : 30 particle : alcohol, ratio) of nanoparticles was prepared and deposited FTO glass was immersed for 5 min., followed by

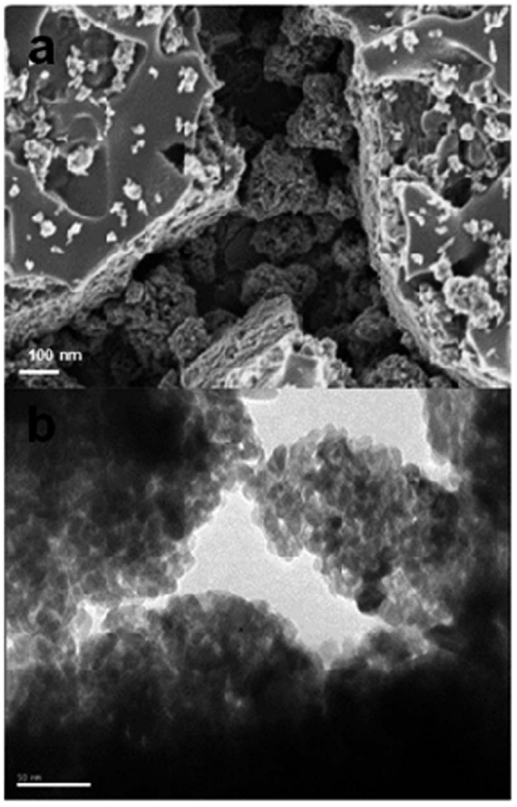

Fig. 4 SEM and TEM images ((a) and (b) respectively) of nanoparticle disposition in intra-particles space.

heating for 5 h at 250 °C. The SEM image in Fig. 4 describes that nanoparticles were mainly deposited in the intra-particles space and filled-up very well. This approach will not only increase the surface area but also amount of dye while fabrication of solar devices. TEM images demonstrate the highly distributed oval shaped anatase form of TiO_2 of 5–10 nm diameters. The dominant peak of (101) in XRD spectra for this sample, further confirmed the formation of anatase form. At low temperatures many nucleation centers should be present on the substrate leading the formation of small crystals of less agglomeration and for short time of annealing at lower temperature may not allow the growth of small crystal into bigger size. The mechanism of bio-templating is presented in the Fig. 5. The milky TTP sol converted transparent after heating for 6 h, due to formation of nano-colloids by hydrolysis in presence of water. With time of heating, water goes off and TTP balance this requirement by associating with bonded water layers around cellulose chains. The nanoparticles forms and connected with each other in compact fashion by covering the cellulose chains. The coverage of surface was confirmed in SEM micrograph (Fig 5i) where stacked nanoparticles in the form of agglomerated blocks were visible on the surface of cellulose, attributed to the drying of specimens during SEM. Results obtained by FT-IR spectroscopy of samples[23] (Fig 5ii) exhibited hump between 3200 and 3600 cm^{-1} is responsible for the hydroxyl group of cellulose. The peaks at 1000–1300 cm^{-1}, for –C–OH stretching and C–OC bending were weak attributed to the growing of nanoparticles on the cellulose surface. A clear and drastic decrease at 1650 cm^{-1} for carbonyl group (–C=O)[23] was additional conformation of strong interaction between metal–O–C and OH– of cellulose.

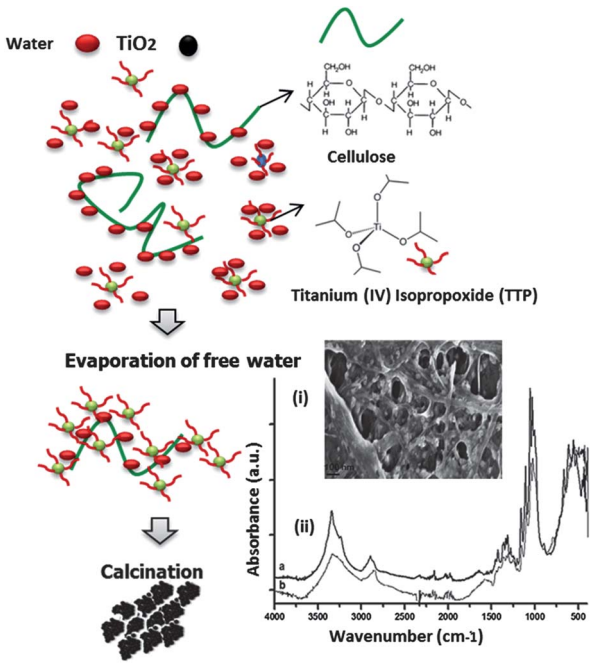

Fig. 5 Mechanism of templating. (i) & (ii) are SEM images and FT-IR spectra of suspension of TTP and BC. (a) & (b) in FT-IR represent the spectra of pure BC and after TTP-BC drying.

The observation of C–H stretching at 2915 cm^{-1} exhibited that in the suspension of cellulose and TTP metal oxide particles were attempting to adhere on the cellulose surface inhibiting the penetration of proper frequency waves required for dipole moment during FT-IR measurements. Analysis suggests that after adherence on the surface, TTP should try to move toward coiled portion of nanofibers (hydro dynamic volume) and need to clear the obstacle of diffusion resistance caused by twisting. At high temperate of calcination, nanoparticles were deposited in blocks due to decomposition of cellulose chains. Cellulose decomposition was confirmed by Thermogravimetric analysis, where 3 main peaks were observed at 90 °C attributed to adsorbed water, 210 °C for any remaining traces of non-cellulosic material, followed by removal of cellulose between 480 and 500 °C. The mechanism was further supported by an additional experiment where larger size of agglomerated particles and intra particle space were generated by templating with concentrated suspension of cellulose nanofibers (5 wt%).

Therefore, if the concentration of cellulose nanofibers is high, the available water molecules are low for the TTP due to higher interconnection among cellulose chains and TTP should require more energy to penetrate that network, forcing higher number of nanoparticles to get agglomerates and grow in the larger size.

Conclusions

Nanoparticles were deposited directly on the FTO glass by sol–gel process, followed by the filling of micro-meter intra-particle gaps with commercial TiO_2. The ribbon shaped nano-dimensional cellulose nanofibers assisted the deposition by fabricating ordered structure of highly uniform thickness at very lower concentration. Deposition was governed by the presence of bonded water molecules on the hydrophilic surface of bacterial cellulose nanofiber that attract the nano-colloids for hydrolysis reaction and generation of nanoparticles. The present approach has potential to increase the efficiency of solar dependent dye sensitised energy storage devices as they required the higher amount of absorbed dye for sensitization as well as intra-particle spacing for adequate scattering.

Acknowledgements

Brain pool fellowship (KOFST), National Research Foundation of Korea (NRF) grant funded by the Republic of Korea government (MEST) (no. NRF-2010-0029227) and Research Foundation of Korea (NRF) grant funded by the Korea government (MEST) (no. 2012047189) are gratefully acknowledged for financial support during the research.

Notes and references

1 (*a*) J. Cui, W. He, H. Liu, S. Liao and Y. Yue, *Colloids Surf., B*, 2009, **74**, 274; (*b*) Z.-Z. Gu, R.-Q. Zhang, G.-Z. Han, C. Pan, H. Zhang, X. J. Tian and Z. M. Chen, *Appl. Phys. Lett.*, 2005, **86**, 201915; (*c*) T. Yui, Y. Mori, T. Tsuchino, T. Itoh, T. Hattori, A. Fukushima and K. Takagi, *Chem. Mater.*,

2005, **17**, 206; (*d*) B. Zhang, S. A. Davis, N. H. Mendelson and S. Mann, *Chem. Commun.*, 2000, 781; (*e*) Y. Shin, J. Liu, J. Chang, H. Z. Nie and G. J. Exarhos, *Adv. Mater.*, 2001, **13**, 728; (*f*) A. T. Raghavender, A. P. Samantilleke, P. Sa, B. G. Almeida, M. I. Vasilevskiy and N. H. Hong, *Mater. Lett.*, 2012, **69**, 59.

2 X. F. Li, T. X. Fan, H. Zhou, S. K. Chow, W. Zhang, D. Zhang, Q. X. Guo and H. Ogawa, *Adv. Funct. Mater.*, 2009, **19**, 45.

3 H. L. Su, Q. Dong, J. Han, D. Zhang and Q. X. Guo, *Biomacromolecules*, 2008, **9**, 499.

4 (*a*) J. H. Li, X. Y. Shi, L. J. Wang and F. Liu, *J. Colloid Interface Sci.*, 2007, **315**, 230; (*b*) D. Yang, L. Qi and J. Ma, *Adv. Mater.*, 2002, **14**, 1543.

5 S. A. Davis, S. L. Burkett, N. H. Mendelson and S. Mann, *Nature*, 1997, **385**, 420.

6 G. Cook, P. L. Timms and C. Goeltner-Spickermann, *Angew. Chem., Int. Ed.*, 2003, **42**, 557.

7 S. R. Hall, H. Bolger and S. Mann, *Chem. Commun.*, 2003, 2784.

8 Y. Shin, C. Wang and G. J. Exarhos, *Adv. Mater.*, 2005, **17**, 73.

9 F. C. Meldrum and R. Seshadri, *Chem. Commun.*, 2000, 29.

10 D. Zhang and L. Qi, *Chem. Commun.*, 2005, 2735.

11 J. Gutierrez, S. C. M. Fernandes, I. Mondragon and A. Tercjak, *Cellulose*, 2013, **20**, 1301.

12 D. Sun, J. Yang and X. Wang, *Nanoscale*, 2010, **2**, 287.

13 J. Huang, T. Kunitake and J. Am, *Chem. Soc.*, 2003, **125**, 11834.

14 (*a*) J. K. Pandey, S. H. Ahn, C. S. Lee, A. K. Mohanty and M. Mishra, *Macromol. Mater. Eng.*, 2010, **295**, 975; (*b*) J. K. Pandey, H. Takagi, D. R. Saini, A. N. Nakagaito and S. H. Ahn, *Composites, Part B*, 2012, **43**, 2822.

15 D. Klemm, D. Schumann, U. Udhardt and S. Marsch, *Prog. Polym. Sci.*, 2001, **26**, 1561.

16 E. T. Reese, R. G. H. Siu and H. S. Levinson, *J. Bacteriol.*, 1950, **59**, 485.

17 B. Laskiewicz, *J. Appl. Polym. Sci.*, 1998, **67**, 1871.

18 S. Yamanaka, K. Watanabe, N. Kitamura, M. Iguchi, S. Mitsuhashi, Y. Nishi and M. Uryu, *J. Mater. Sci.*, 1989, **24**, 3141.

19 (*a*) M. Rehan, X. Lai and G. M. Kale, *CrystEngComm*, 2011, **13**, 3725; (*b*) W. Guo, Y. Shen, G. Boschloo, A. Hagfeldt and T. Ma, *Electrochim. Acta*, 2011, **56**, 4611; (*c*) R. K. Reyes-Gil, A. E. Reyes-García and D. Raftery, *J. Electrochem. Soc.*, 2006, **153**, A1296.

20 J. H. Bang and P. V. Kamat, *Adv. Funct. Mater.*, 2010, **20**, 1970.

21 K. Okada, N. Yamamoto, Y. Kameshima and A. Yasumori, *J. Am. Ceram. Soc.*, 2001, **84**, 159.

22 (*a*) Y. Lee and M. Kang, *Mater. Chem. Phys.*, 2010, **122**, 284; (*b*) C. Y. Huang, Y. C. Hsu, J. G. Chen, V. Suryanarayanan, K. M. Lee and K. C. Ho, *Sol. Energy Mater. Sol. Cells*, 2006, **90**, 2391; (*c*) C. S. Karthikeyan, M. Thelakkat and M. Willert-Porada, *Thin Solid Films*, 2006, **511**, 187.

23 (*a*) H. S. Qian, M. Antonietti and S. H. Yu, *Adv. Funct. Mater.*, 2007, **17**, 637; (*b*) C. Wang, E. Y. Yan, Z. H. Huang, Q. Zhao and Y. Xin, *Macromol. Rapid Commun.*, 2007, **28**, 205; (*c*) M. Kacuráková, A. C. Smith, M. J. Gidley and R. H. Wilson, *Carbohydr. Res.*, 2002, **337**, 1145.